



TITLE:

<Division of Synthetic Chemistry>Advanced Inorganic Synthesis

AUTHOR(S):

CITATION:

<Division of Synthetic Chemistry>Advanced Inorganic Synthesis. ICR Annual Report 2018, 25: 10-11

ISSUE DATE:

2018

URL:

<http://hdl.handle.net/2433/240675>

RIGHT:

Copyright © 2019 Institute for Chemical Research, Kyoto University

Division of Synthetic Chemistry

– Advanced Inorganic Synthesis –

http://www.scl.kyoto-u.ac.jp/~teranisi/index_E.html



Prof
TERANISHI, Toshiharu
(D Eng)



Assoc Prof
SAKAMOTO, Masanori
(D Eng)



Assist Prof
SATO, Ryota
(D Sc)



Program-Specific Assist Prof
SARUYAMA, Masaki
(D Sc)



Program-Specific Assist Prof
TRINH, Thang Thuy
(Ph D)



PD
KAWAWAKI, Tokuhisa
(D Eng)



PD
EGUCHI, Daichi
(D Sc)



PD
TAKAHATA, Ryo
(D Sc)



PD
LIU, Ming-Han
(Ph D)



PD
XUE, Songlin
(D Sc)



PD
LIAN, Zichao
(D Sc)

Students

KIM, Sungwon (D3)

MATSUMOTO, Kenshi (D3)

ZHANG, Jie (D2)

OKAMOTO, Yasuo (D1)

LI, Zhanzhao (D1)

SHAKUDO, Hikaru (M2)

WATANABE, Yuki (M2)

KANEKO, Ryota (M1)

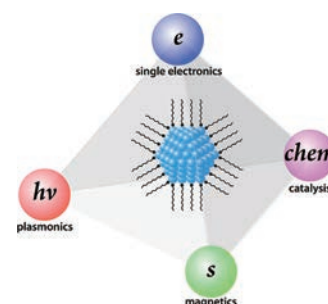
GAO, Jingying (RS)

Scope of Research

We are focusing on the precise synthesis of inorganic nanoparticles by controlling the primary (size, shape, composition, etc.) and secondary (spatial arrangement) structures to tune properties such as electron confinement, carrier oscillation, spin, and catalysis. These high-quality inorganic nanoparticles are applied to both high-performance nanodevices (e.g., single electron transistor, plasmon waveguide, and nanocomposite magnet) and photo-energy conversion materials (e.g., overall water splitting and solar cell).

KEYWORDS

Inorganic Nanoparticles Single Electronics Plasmonics
Nanocomposite Magnet Photocatalysts



Selected Publications

Saruyama, M.; Kim, S.; Nishino, T.; Sakamoto, M.; Haruta, M.; Kurata, H.; Akiyama, S.; Yamada, T.; Domen, K.; Teranishi, T., Phase-Segregated $\text{NiP}_x\text{@FePyO}_z$ Core@Shell Nanoparticles: Ready-to-Use Nanocatalysts for Electro- and Photo-Catalytic Water Oxidation through in-situ Activation by Structural Transformation and Spontaneous Ligand Removal, *Chem. Sci.*, **9**, 4830-4836 (2018).

Lian, Z.; Sakamoto, M.; Matsunaga, H.; Vequizo, J. J. M.; Yamakata, A.; Haruta, M.; Kurata, H.; Teranishi, T., Near Infrared Light Induced Plasmonic Hot Hole Transfer at a Nano-Heterointerface, *Nat. Commun.*, **9**, 2314 (2018).

Eguchi, D.; Sakamoto, M.; Teranishi, T., Ligand Effect on the Catalytic Activity of Gold Clusters in the Electrochemical Hydrogen Evolution Reaction, *Chem. Sci.*, **9**, 261-265 (2018).

Near Infrared Light Induced Plasmonic Hot Hole Transfer at a Nano-Heterointerface

Localized surface plasmon resonance (LSPR)-induced photoenergy conversion is among the great challenges causing a paradigm shift in both scientific fields and industry regarding solar-energy utilization. Although plasmonic materials have superior light-harvesting abilities, the low conversion efficiency caused by ultrafast relaxation of the hot carrier and charge recombination is a major drawback. Furthermore, the unclear behavior of hot holes becomes an obstacle for the comprehensive understanding of LSPR-induced carrier transfer.

Herein, we elucidate the LSPR-induced behavior of hot holes in plasmonic CuS NCs and CdS/CuS HNCs using time-resolved infrared (TR-IR) spectroscopy. We discover that a multi-step carrier transfer (plasmon-induced transit carrier transfer: PITCT) realized efficient hole transfer from the CuS phase to the CdS phase. Surprisingly, the PITCT of CdS/CuS HNCs achieves high quantum yields (19%) and long-lived charge separation (9.2 μ s). Because ultrafast charge recombination is a major drawback of all plasmonic energy conversion systems, the PITCT mechanism proposed here should change the conventional consensus regarding LSPR-induced energy conversion.

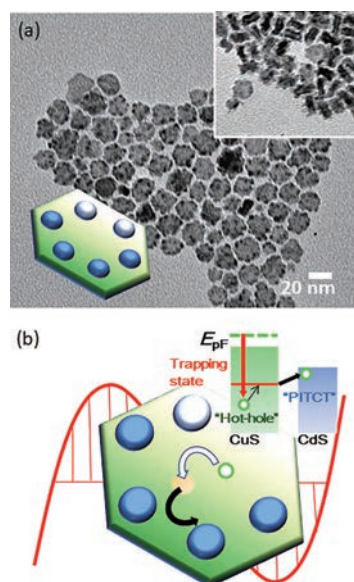


Figure 1. (a) TEM images of CdS/CuS HNCs. (b) Schematic illustration of PITCT (plasmon-induced transit carrier transfer) mechanisms.

Phase-Segregated $\text{NiP}_x@ \text{FeP}_y\text{O}_z$ Core@Shell Nanoparticles: Ready-to-Use Nanocatalysts for Electro- and Photo-Catalytic Water Oxidation

Production of H_2 and O_2 by efficient and sustainable electrolysis of water is important for the technology of

noble clean energy such as solar-driven fuel generating system. In the water splitting reaction, the oxygen evolution reaction (OER) is considered to be bottle-neck because OER typically requires 4 electrons for O-O bond formation, which is a kinetically slow process. A high overpotential is required for OER in spite of using low abundance and high cost novel metals, such as Ir or Ru, which inhibit the water electrolysis device from the global scalability.

For the purpose of the creation of earth abundant and efficient electrocatalyst for OER, we synthesized nickel phosphide (NiP_x)@iron phosphate (FeP_yO_z) core@shell nanoparticles (NPs). NiP_x -seed-mediated growth method allowed FeP_yO_z to grow onto the NiP_x NPs selectively (Figure 2a). $\text{NiP}_x@ \text{FeP}_y\text{O}_z$ core@shell NP has crystalline NiP_x core with sphere-with-rod morphology, and amorphous FeP_yO_z shell. $\text{NiP}_x@ \text{FeP}_y\text{O}_z$ NPs loaded carbon catalyst exhibited low overpotential of 0.28 V at 10 mA cm^{-2} in 0.1 M KOH solution. Furthermore, photoelectrochemical measurements showed that the photocurrent of BiVO_4 was greatly enhanced by simple deposition of $\text{NiP}_x@ \text{FeP}_y\text{O}_z$ NPs on BiVO_4 electrode (Figure 2b). This $\text{NiP}_x@ \text{FeP}_y\text{O}_z$ NPs can be used as ready-to-use OER catalyst without any post treatments such as annealing, because an in-situ transformation into Ni-Fe hydroxide active species. This feature is a considerable advantage of our catalytic NPs in the fabrication of large scale electro- and photocatalytic systems.

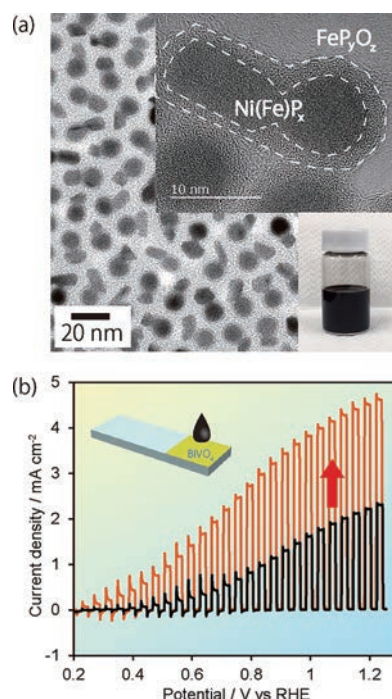


Figure 2. (a) TEM images of $\text{NiP}_x@ \text{FeP}_y\text{O}_z$ core@shell NPs and the picture of their hexane solution. (b) Photo current measurement of water oxidation using (black) bare and (orange) $\text{NiP}_x@ \text{FeP}_y\text{O}_z$ core@shell NPs deposited BiVO_4 photoanodes in 0.125 M $\text{K}_2\text{B}_4\text{O}_7$ electrolyte.